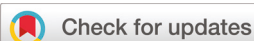


COMMUNICATION


 Cite this: *Analyst*, 2020, **145**, 5113

Received 8th April 2020,

Accepted 8th June 2020

DOI: 10.1039/d0an00704h

rsc.li/analyst

A new method to amplify colorimetric signals of paper-based nanobiosensors for simple and sensitive pancreatic cancer biomarker detection†

 K. Sudhakara Prasad,^{‡a} Yousef Abugalyon,^a Chunqiang Li,^b Feng Xu^{‡c} and XiuJun Li^{‡*a,d}

A low-cost, sensitive, and disposable paper-based immunosensor for instrument-free colorimetric detection of pancreatic cancer biomarker PEAK1 was reported for the first time by capitalizing the catalytic properties of gold nanoparticles in colour dye degradation. This simple signal amplification method enhances the detection sensitivity by about 10 fold.

Early detection of a disease biomarker is crucial to the timely treatment of diseases.¹ There is an urgent need for rapid monitoring of disease biomarkers for cancer, a non-communicable disease that contributes a large number for the increasing global mortality.^{2,3} According to the World Health Organization, there are 8.8 million people who died worldwide due to cancer,⁴ and the current data from the American Cancer Society forecast 1 688 780 new cases of cancer and 600 920 deaths in the US.⁵ 57% percent of new cancer cases arise in developing nations and the figure could reach 70% by 2050.^{6,7} Their cancer mortality now accounts for 70% of cancer deaths worldwide.^{7–11} Among these cancer cases, pancreatic cancer caused an estimated number of 43 090 deaths in the US in 2017. Pancreatic cancer mostly occurs in the exocrine pancreas, namely pancreatic ductal adenocarcinoma (PDAC). PDAC is the fourth-leading cause of cancer death in the US, and the incidence of PDAC is increasing compared to other types of cancer.^{5,12–14} Since the pancreas is deep inside the

body, regular screening may not identify the early progression of such a tumour. Additionally, the lack of symptoms at early stages makes the tumour difficult to be identified. The appearance of symptoms after PDAC spreads to other organs further decreases the 5-year survival rate to approximately 5%.¹⁵ Therefore, a low-cost method for rapid and reliable early diagnosis of PDAC is in great need.

Recently, Kelber *et al.* discovered that a novel tyrosine kinase, PEAK1 (pseudopodium-enriched atypical kinase one, SGK269), could be used as a biomarker for PDAC.¹³ Developing an immunosensor for PEAK1 that fulfills the conditions of a point-of-care tool with simple, sensitive, portable, rapid, low-cost and miniature features will be of great importance for the early clinical diagnosis of PDAC. However, traditional immunoassay methods with various sensing strategies such as radiation,¹⁶ fluorescence,^{17,18} surface plasmon resonance (SPR),^{19,20} quartz crystal microbalance,²¹ well-known enzyme-linked immunosorbent assays (ELISA),^{22,23} chemiluminescence²⁴ and electrochemistry^{25–28} require complex, expensive instruments and skilled operators. Furthermore, conventional methods including tissue immunohistochemistry and western blotting for PEAK 1 measurement are invasive, cumbersome, and costly, and they can only provide semi-quantitative results.^{29,30} Although electrochemical detection can provide quantitative data, it requires an expensive potentiostat, creating a challenge for point-of-care detection.²⁸ Considering these hindrances, a much simpler paper-based colorimetric assay method shows potential for low-cost point-of-care detection of the PDAC biomarker PEAK1, because of its simplicity, low cost, requirement of a low volume of sample, and disposable nature.^{23,31–40}

Gold nanoparticles (AuNPs) with 10–50 nm diameter are commonly used in various colorimetric assays and exhibit red colour in a dispersed state and present a purple or blue colour in an aggregated state due to their interparticle distance and size-dependent localized surface plasmon resonance.^{38,41} However, due to low sensitivity resulting from poor signal amplification, signal enhancement techniques such as enzyme

^aDepartment of Chemistry, University of Texas at El Paso, 500 West University Avenue, El Paso, Texas, 79968, USA. E-mail: xli4@utep.edu; Fax: +1-915-747-5748; Tel: +1-915-747-8967

^bDepartment of Physics, Border Biomedical Research Center, University of Texas at El Paso, 500 West University Avenue, El Paso, Texas, 79968, USA

^cBioinspired Engineering & Biomechanics Center (BEBC), Xi'an Jiaotong University, Shaanxi, P. R. China

^dBiomedical Engineering, Border Biomedical Research Center, and Environmental Science & Engineering, University of Texas at El Paso, USA

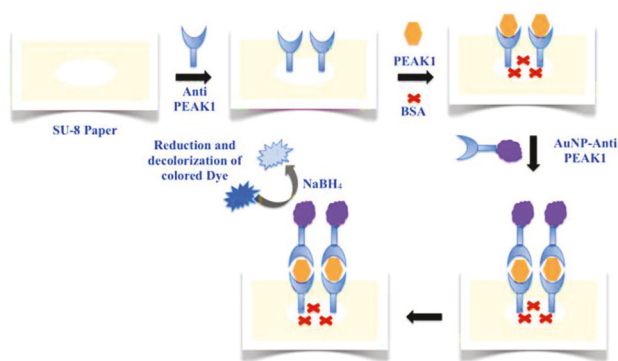
† Electronic supplementary information (ESI) available: Materials and chemicals list and preparation of the AuNP bioconjugate. See DOI: 10.1039/d0an00704h

‡ Current affiliation: Yenepoya Research Centre, Yenepoya (Deemed to be University) University Road, Mangalore-575018, Karnataka, India.

cascade reactions or silver enhancement are often needed to enhance the sensitivity.^{42,43} Yet the use of enzymes and growth of palladium nanostructures on the surface of AuNPs make the assay fairly complex. Taking advantage of the enzyme-like catalytic properties of AuNPs,^{44–46} herein, we report for the first time a new method to amplify the colorimetric signals based on catalytic activities of AuNPs towards azo dye degradation and have developed a novel disposable colorimetric immunosensor for the rapid POC detection of the PDAC biomarker PEAK1 on a paper-based microfluidic device.

Scheme 1 shows the main principle and procedures of the colorimetric detection of PEAK1 by the paper-based nano-immunosensor, based on the AuNP-catalyzed reduction of a colour dye. In this work, the immunosensor for PEAK1 was fabricated using the photolithography technique on SU-8-treated chromatographic paper with detection zones (2 mm diameter),^{33,47} following each step in Scheme 1. First, paper detection zones were treated with 2 μL PEAK1 capture antibodies, anti PEAK1 (20 $\mu\text{g mL}^{-1}$ in phosphate buffered saline, PBS), for 20 minutes and subsequently washed with PBS. Then, after the paper surface was blocked with a 0.5% BSA solution, 2 μL of different concentrations of PEAK1 were added and incubated for 15 minutes to facilitate immunorecognition, followed by washing with PBS to remove the unbound PEAK1. Next, the bioconjugate probes, AuNP-tagged anti PEAK1 bioprobes, were added onto the paper surface and incubated for another 20 minutes to establish a sandwich-structure immunocomplex. Finally, hydroxy naphthol blue (HNB) in the presence of NaBH_4 was added to amplify the signal for sensitive colorimetric detection, in which AuNPs catalyzed the degradation of azo dyes (*i.e.* HNB) in the presence of NaBH_4 and resulted in color changes.^{45,48–51}

Before the colorimetric signal amplification step, we first tested the AuNP-based colorimetric detection of PEAK1 as a comparison (*i.e.* without signal amplification), as shown in Fig. 1. When adding different concentrations of the target PEAK1 to different detection zones (10^{-6} , 10^{-8} , and 0 g mL^{-1} PEAK1 for Fig. 1A(a)–(c), respectively), the immunocomplex showed different colours. The colour change was attributed to



Scheme 1 Schematic depiction of the colorimetric detection of PEAK1 by paper-based nano-immunosensors, based on the AuNP-catalyzed reduction of colour dye by NaBH_4 .

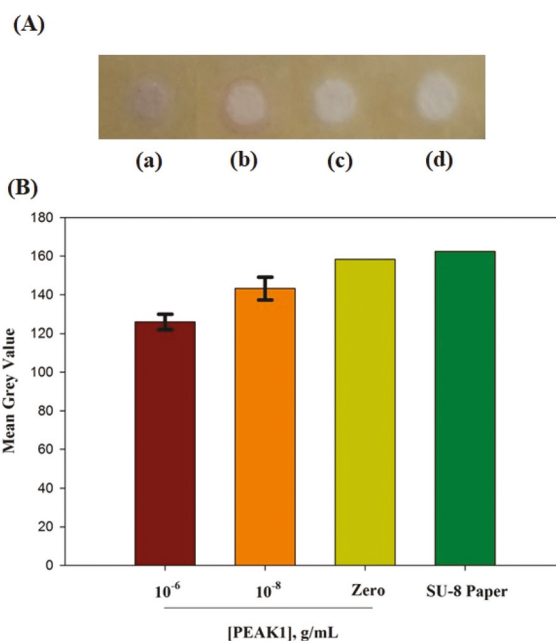


Fig. 1 Images (A) and gray values (B) of SU-8-treated paper detection zones (2 mm diameter) with (a) 10^{-6} , (b) 10^{-8} , and (c) 0 g mL^{-1} PEAK1, and (d) SU-8 paper detection zones before any immunoassay procedures.

different amounts of AuNP bioprobes bound to different concentrations of PEAK1 during the immunorecognition. The absence of PEAK1 protein exhibited no colour change in the detection zones (Fig. 1A(c)), while the presence of 10^{-6} and $10^{-8} \text{ g mL}^{-1}$ PEAK1 caused a purple colour (Fig. 1A(a)) and a light pink colour (Fig. 1A(b)), respectively, due to the SPR optical properties of AuNPs.³⁸ These colour changes demonstrated that AuNP-tagged anti PEAK1 bioprobes could be used for the development of a colorimetric PEAK1 sensor. Nevertheless, the obscure color change in low concentrations of PEAK1 made it difficult for sensitive quantification of PEAK1 protein.

To solve this impediment, we capitalized the catalytic properties of AuNPs to amplify colorimetric signals. To confirm the feasibility to use the developed immunoprobe for the degradation of an azo dye, and thus to develop a sensitive colorimetric immunosensor, we first studied the effects of the immunoprobe on an azo dye, hydroxy naphthol blue (HNB), in the presence of NaBH_4 .

UV-vis absorption spectra studies were carried out with a Beckman Coulter DU 730 UV spectrometer to clarify the importance of the immunoprobe in the degradation of HNB. As shown in Fig. 2, HNB exhibited well-defined absorption peaks centred at 600 and 645 nm (curve (a) in Fig. 2A). After the addition of 0.1 M NaBH_4 (curve (b) in Fig. 2A), no typical change in the absorption spectra was noticed (*i.e.* the same absorption peaks centred at 600 and 645 nm), which indicates that the reduction of HNB did not occur (note that the absorbance in the y-axis was offset for easy comparison). Interestingly, even after keeping the mixture for a long period

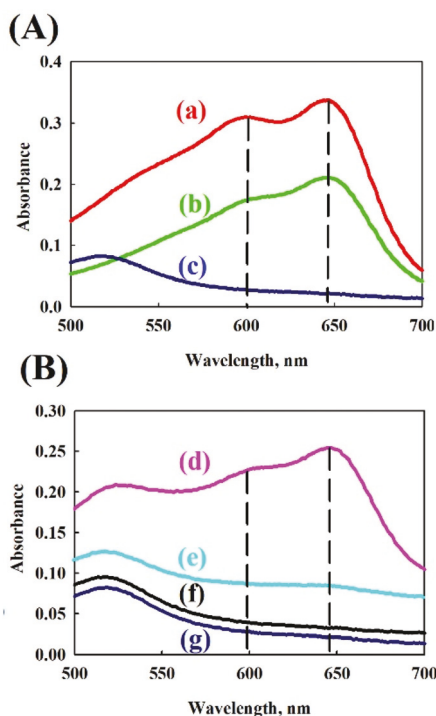


Fig. 2 (A) UV-vis absorption spectra of (a) HNB, (b) HNB with NaBH₄, and (c) HNB + NaBH₄ + AuNP-anti PEAK1 after 30 minutes. (B) UV-vis absorption spectra (d–g) at 0, 5, 30, and 40 minutes after the addition of AuNP-anti PEAK1 to the mixture of HNB and NaBH₄, respectively.

of time, no changes were observed. The obtained results are similar to those in a previous report by Li *et al.*,⁴⁵ in which the addition of NaBH₄ failed to promote the degradation of an azo dye (methyl orange). In contrast, in the presence of AuNP-anti PEAK1, the absorption peaks of HNB disappeared gradually as the reaction proceeded in Fig. 2A(c). We further studied the spectra of the mixture of HNB + NaBH₄ at different times after adding AuNP-anti PEAK1. It can be found from Fig. 2B that the complete degradation of HNB (disappearance of the HNB absorption peak) took place after 5 minutes (Fig. 2B(e)). This clearly indicated that HNB was degraded in the presence of AuNP-tagged immunoprobes, and AuNP-anti PEAK1 indeed exhibited good catalytic properties. Thus, AuNP-catalyzed degradation of HNB can be used as a colorimetric indicator for PEAK1 detection.

To demonstrate the aforementioned proof-of-concept for the POC detection of PEAK1, we dropped coated HNB onto paper detection zones and dried it at room temperature. As shown in Fig. 3A and B, HNB produced a purple colour, and in the presence of NaBH₄ it turned sky blue, which was probably attributed to the change of the pH value since NaBH₄ is a base. When there was zero g mL⁻¹ PEAK1, the light blue colour remained the same (Fig. 3A), whether there was NaBH₄ or not. However, it is interesting to note that the colour changed from light blue to colourless, when 10⁻⁶ g mL⁻¹ PEAK1 was added onto complete immunosensor detection zones constructed by following the immunoassay steps

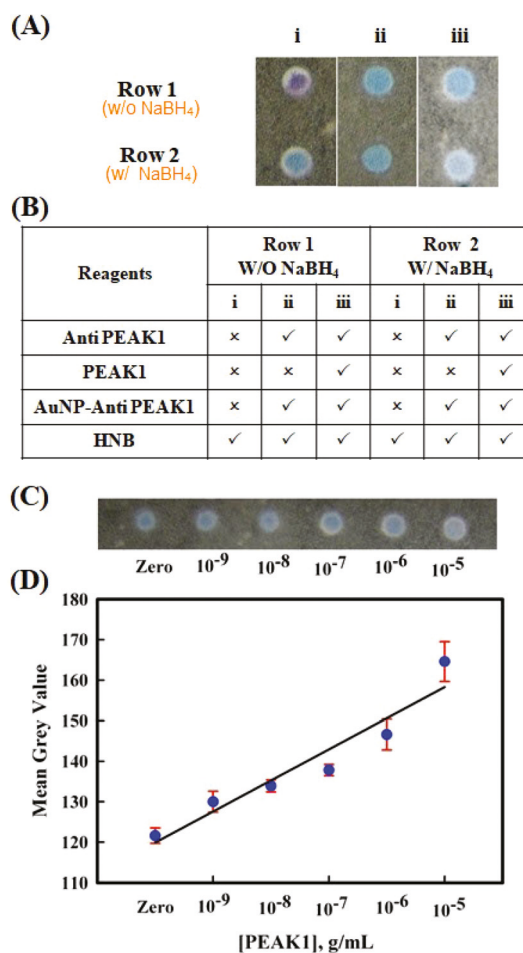


Fig. 3 (A and B) Images for the reactions between (i) HNB, (ii) HNB + zero g mL⁻¹ PEAK1 sandwich immunocomplex, and (iii) HNB + 10⁻⁶ g mL⁻¹ PEAK1 sandwich immunocomplex in the absence (top row) or in the presence (bottom row) of NaBH₄ on paper detection zones. (C) Images and (D) the calibration curve of the paper-based immunosensor for the colorimetric detection of different concentrations of PEAK1.

depicted in Scheme 1, in the presence of HNB and NaBH₄. The colour change was mainly due to the catalytic degradation of the colour of HNB in the presence of NaBH₄ by AuNPs from the immunocomplex which was confirmed by XPS (Fig. S1†). In contrast, as for zero g mL⁻¹ PEAK1, there were no AuNP-anti PEAK1 for the immunorecognition and no AuNPs to bleach the dye, resulting in no colour change. This indicates the feasibility of using AuNP-catalyzed degradation of HNB for the colorimetric detection of biomolecules.

After the feasibility test, different concentrations of PEAK1 ranging from zero to 10⁻⁶ g mL⁻¹ PEAK1 were tested using the paper-based nano-immunosensor catalyzed by AuNPs for colorimetric detection. The colour changes from blue (zero g mL⁻¹ PEAK1) to colorless (10⁻⁶ g mL⁻¹ PEAK1) at different concentrations of PEAK1 (Fig. 3C) could be recognized by the naked eye. Nevertheless, to obtain quantitative data, we measured the grey values of digitally photographed detection zones with different concentrations of PEAK1 using ImageJ

software.^{52–54} It can be clearly observed from Fig. 3D that the grey intensity values increased gradually as the concentrations of PEAK1 varied from low (10^{-9} g mL⁻¹) to high (10^{-5} g mL⁻¹). The calibration plot exhibited a linear range between 10^{-5} and 10^{-9} g mL⁻¹ PEAK1, with a squared correlation coefficient of 0.975. As mentioned earlier, the degradation of HNB was directly proportional to the amount of AuNP-anti PEAK1 bound to different concentrations of PEAK1 during the formation of the sandwich immunoassay on the paper-based device. With increased concentration of PEAK1, the AuNPs present on the detection zones increased accordingly, which facilitated the decolourization of HNB. The limit of detection (LOD) was calculated to be 1.0 ng mL⁻¹ PEAK1 by considering three times the standard deviation above the blank. This LOD was about 10-fold lower than that of AuNP-based colorimetric detection without signal amplification, indicating higher detection sensitivity of our new AuNP-catalyzed colorimetric immunoassay.

In conclusion, we have developed a novel, cost-effective, and simple paper-based colorimetric immunoassay method for the sensitive detection of a pancreatic cancer biomarker, PEAK1, by utilizing the catalytic activity of AuNPs in decolourization of a coloured azo dye without employing an enzyme or the Ag and Au enhancement technique for signal amplification. This AuNP-catalyzed colorimetric immunoassay on a paper-based device can detect 1.0 ng mL⁻¹ level of PEAK1 in an hour, which enhances the detection sensitivity by 10 fold than an AuNP-based colorimetric immunoassay without signal amplification (LOD of ~ 10.0 ng mL⁻¹ PEAK1). This method is also simpler and faster than conventional ELISA techniques that require long time (*e.g.* about 30 hours⁵⁵) and sophisticated instruments, and thus it could be used for the early diagnosis of PDAC at the point of care. Along with (I) faster assays from paper-based devices, some other major benefits of paper-based devices in this work include: (II) it is a low-cost platform and (III) the white colour of paper makes the device usually have low background and high contrast in colour changes, thus making it highly suitable for colorimetric detection. In addition, the proposed detection technique can be used for the development of other biosensing methods for point-of-care diagnosis from different biological specimens. To address the issue of interference from blood, the incorporation of blood filtration membranes or plasma separation membranes onto a paper-based device will facilitate circumventing colour interference in colorimetric assays.^{56,57}

Conflicts of interest

There are no conflicts to declare.

Acknowledgements

We are grateful for the financial support from the Philadelphia Foundation, the Medical Center of the Americas Foundation,

the U.S. NSF-PREM program (DMR 1827745), and the UTEP IDR program. Financial support to our research from the National Institute of General Medical Sciences of the NIH (SC2GM105584), the National Institute of Allergy and Infectious Disease of the NIH (R21AI107415), NSF I-Corps (IIP1953841), the NIH RCMI Pilot grant (5G12MD007593-22), and the University of Texas (UT) System for the STARS award is also greatly acknowledged. We also thank Dr Qunqun Guo for the help in the manuscript preparation and the NIH BUILDing Scholar program for the support to YA.

Notes and references

- 1 S. T. Sanjay, G. Fu, M. Dou, F. Xu, R. Liu, H. Qi and X. Li, *Analyst*, 2015, **140**, 7062–7081.
- 2 C. D. Mathers and D. Loncar, *PLoS Med.*, 2006, **3**, 442–449.
- 3 P. Kanavos, *Ann. Oncol.*, 2006, **17**, viii15–viii23.
- 4 WHO, <http://www.who.int/cancer/en/>.
- 5 Cancer facts & figures 2017, <https://www.cancer.org/content/dam/cancer-org/research/cancer-facts-and-statistics/annual-cancer-facts-and-figures/2017/cancer-facts-and-figures-2017.pdf>.
- 6 Most of the world's cancer cases are now in developing countries, <https://www.npr.org/sections/goatsandsoda/2015/12/15/459827058/most-of-the-worlds-cancer-cases-are-now-in-developing-countries>, 2019.
- 7 J. Frenk, Cancer is on the rise in developing nations, <http://www.hsph.harvard.edu/news/magazine/shadow-epidemic/>, accessed Feb 20, 2016.
- 8 WHO, Cancer in developing countries: facing the challenge, http://www.who.int/dg/speeches/2010/iaea_forum_20100921/en/, accessed Feb. 20, 2016.
- 9 Cancer facts & figures 2017, 1- <https://www.cancer.org/research/cancer-facts-statistics/all-cancer-facts-figures/cancer-facts-figures-2017.html>.
- 10 <http://www.who.int/cancer/en/>.
- 11 <https://geo.iarc.fr/today/data/factsheets/cancers/13-Pancreas-fact-sheet.pdf>.
- 12 A. H. Al Haddad and T. E. Adrian, *Expert Opin. Invest. Drugs*, 2014, **23**, 1499–1515.
- 13 J. A. Kelber, T. Reno, S. Kaushal, C. Metildi and R. L. Klemke, *Cancer Res.*, 2012, **72**, 2554–2564.
- 14 E. Collisson and M. Tempero, *Clin. Cancer Res.*, 2011, **17**, 203–205.
- 15 M. Hidalgo, *N. Engl. J. Med.*, 2010, **362**, 1605–1617.
- 16 J. E. Causse, I. Ricordel, M. N. Bachelier, F. Kaddouche, B. Nom, R. Weil, B. Descomps and J. P. Yver, *Clin. Chem.*, 1990, **36**, 525–533.
- 17 J. Tang, D. Tang, R. Niessner, G. Chen and D. Knopp, *Anal. Chem.*, 2011, **83**, 5407–5414.
- 18 L. Liu, X. Dong, W. Lian, X. Peng, Z. Liu, Z. He and Q. Wang, *Anal. Chem.*, 2010, **82**, 1381–1388.
- 19 E. N. M. Schelhaas, N. Kuder, B. Bader, J. Kuhlmann, A. Wittinghofer and H. Waldmann, *Chem. – Eur. J.*, 2015, **5**, 1239–1252.

- 20 K. Stembera, S. Vogel, A. Buchynskyy, J. A. Ayala and P. Welzel, *ChemBioChem*, 2002, **3**, 559–550.
- 21 E. K. Yun, T. Haruyama, M.-L. Laukkanen, K. Keinanen and M. Aizawa, *Anal. Chem.*, 1998, **70**, 260–264.
- 22 G. X. Zhou, J. Ireland, P. Rayman, J. Finke and M. Zhou, *Urology*, 2010, **75**, 257–261.
- 23 S. T. Sanjay, M. Dou, J. Sun and X. Li, *Sci. Rep.*, 2016, **6**, 30474.
- 24 Z. Yang, H. Liu, C. Zong, F. Yan and H. Ju, *Anal. Chem.*, 2009, **81**, 5484–5489.
- 25 K. Kerman, N. Nagatani, M. Chikae, T. Yuhi, Y. Takamura and E. Tamiya, *Anal. Chem.*, 2006, **78**, 5612–5616.
- 26 N. A. Martínez, R. J. Schneider, G. A. Messina and J. Raba, *Biosens. Bioelectron.*, 2010, **25**, 1376–1381.
- 27 X. Zheng and C. Li, *Biosens. Bioelectron.*, 2010, **25**, 1548–1552.
- 28 K. S. Prasad, X. Cao, N. Gao, Q. Jin, S. T. Sanjay, G. Henao-Pabon and X. Li, *Sens. Actuators, B*, 2020, **305**, 127516.
- 29 J. A. Kelber, T. Reno, S. Kaushal, C. Metildi, T. Wright, K. Stoletov, J. M. Weems, F. D. Park, E. Mose, Y. Wang, R. M. Hoffman, A. M. Lowy, M. Bouvet and R. L. Klemke, *Cancer Res.*, 2012, **72**, 2554–2564.
- 30 J. Strnadel, S. Choi, K. Fujimura, H. Wang, W. Zhang, M. Wyse, T. Wright, E. Gross, C. Peinado, H. W. Park, J. Bui, J. Kelber, M. Bouvet, K. L. Guan and R. L. Klemke, *Cancer Res.*, 2017, **77**, 1997–2007.
- 31 G. Fu, S. T. Sanjay and X. Li, *Analyst*, 2016, **141**, 3883–3889.
- 32 M. Dou, S. T. Sanjay, M. Benhabib, F. Xu and X. Li, *Talanta*, 2015, **145**, 43–54.
- 33 C. M. Cheng, A. W. Martinez, J. Gong, C. R. Mace and G. M. Whitesides, *Angew. Chem., Int. Ed.*, 2010, **49**, 4771–4774.
- 34 W. Dungchai, O. Chailapakul and C. S. Henry, *Anal. Chim. Acta*, 2010, **674**, 227–233.
- 35 S. J. Vella, P. Beattie, R. Cademartiri, A. Laromaine, A. W. Martinez, S. T. Phillips, K. A. Mirica and G. M. Whitesides, *Anal. Chem.*, 2012, **84**, 2883–2891.
- 36 M. Zhou, M. Yang and F. Zhou, *Biosens. Bioelectron.*, 2014, **55**, 39–43.
- 37 W. Liu, H. Yang, Y. Ding, S. Ge, J. Yu, M. Yan and X. Song, *Analyst*, 2013, **139**, 251–258.
- 38 W. Zhao, M. M. Ali, S. D. Aguirre, M. A. Brook and Y. Li, *Anal. Chem.*, 2008, **80**, 8431–8437.
- 39 A. K. Yetisen, M. S. Akram and C. R. Lowe, *Lab Chip*, 2013, **13**, 2210–2251.
- 40 H. Manisha, P. D. P. Shwetha and K. S. Prasad, in *Environmental, Chemical and Medical Sensors*, Springer, Singapore, 2018, pp. 315–341.
- 41 W. Zhou, K. Hu, S. Kwee, L. Tang, Z. Wang, J. Xia and X. Li, *Anal. Chem.*, 2020, **92**, 2739–2747.
- 42 Z. Gao, L. Hou, M. Xu and D. Tang, *Sci. Rep.*, 2014, **4**, 3966–3973.
- 43 N. R. Jana and J. Y. Ying, *Adv. Mater.*, 2008, **20**, 430–434.
- 44 W. Li, W. Qiang, J. Li, H. Li, Y. Dong, Y. Zhao and D. Xu, *Biosens. Bioelectron.*, 2014, **51**, 219–224.
- 45 W. Li, J. Li, W. Qiang, J. Xu and D. Xu, *Analyst*, 2013, **138**, 760–766.
- 46 C. C. Chang, C. P. Chen, C. H. Lee, C. Y. Chen and C. W. Lin, *Chem. Commun.*, 2014, **50**, 14443–14446.
- 47 W. Zhou, M. Feng, A. Valadez and X. Li, *Anal. Chem.*, 2020, **92**, 7045–7053.
- 48 R. Rajesh, S. S. Kumar and R. Venkatesan, *New J. Chem.*, 2014, **38**, 1551–1558.
- 49 N. Gupta, H. P. Singh and R. K. Sharma, *J. Mol. Catal. A: Chem.*, 2011, **335**, 248–252.
- 50 P. Singh, S. Roy and A. Jaiswal, *J. Phys. Chem. C*, 2017, **121**, 22914–22925.
- 51 W. Zuo, G. Chen, F. Chen, S. Li and B. Wang, *RSC Adv.*, 2016, **6**, 28774–28780.
- 52 M. Dou, N. Macias, F. Shen, J. Dien Bard, D. C. Domínguez and X. Li, *EclinicalMedicine*, 2019, **8**, 72–77.
- 53 M. Dou, S. T. Sanjay, D. C. Dominguez, P. Liu, F. Xu and X. Li, *Biosens. Bioelectron.*, 2017, **87**, 865–873.
- 54 M. Dou, J. Sanchez, H. Tavakoli, J. E. Gonzalez, J. Sun, J. Dien Bard and X. Li, *Anal. Chim. Acta*, 2019, **1065**, 71–78.
- 55 S. Zhang, A. Garcia-D'Angeli, J. P. Brennan and Q. Huo, *Analyst*, 2014, **139**, 439–445.
- 56 T. Songjaroen, W. Dungchai, O. Chailapakul, C. S. Henry and W. Laiwattanapaisal, *Lab Chip*, 2012, **12**(18), 3392–3398.
- 57 S. Vemulapati, E. Rey, D. O'Dell, S. Mehta and D. Erickson, *Sci. Rep.*, 2017, **7**(1), 1–8.

Supporting information

New method to amplify colorimetric signals of paper-based nanobiosensors for simple and sensitive pancreatic cancer biomarker detection

K.Sudhakara Prasad,^{1,a} Yousef Abugalyon,¹ Chunqiang Li,² Feng Xu,³ and XiuJun Li^{1,4*}

¹*Department of Chemistry, University of Texas at El Paso, 500 West University Avenue, El Paso, Texas, 79968, USA. Fax: +1-915-747-5748; Tel: +1-915-747-8967;*

²*Department of Physics, Border Biomedical Research Center, University of Texas at El Paso, 500 West University Avenue, El Paso, Texas, 79968, USA.*

³*Bioinspired Engineering & Biomechanics Center (BEBC), Xi'an Jiaotong University, Shaanxi, P. R. China*

⁴*Biomedical Engineering, Border Biomedical Research Center, and Environmental Science & Engineering, University of Texas at El Paso, USA.*

^a*Current affiliation: Yenepoya Research Centre, Yenepoya University, Mangalore-575018, Karnataka, India*

Corresponding Author: XiuJun Li; E-mail: xli4@utep.edu

Materials and Chemicals

SU-8 was obtained from MicroChem, while PEAK 1 recombinant protein and Anti PEAK1 were obtained from MyBiosource Inc. Whatman #1 Chromatography paper, AuNPs with 20 nm diameters, hydroxy naphthol blue, phosphate-buffered saline, NaBH₄, and bovine serum albumin were purchased from Sigma and used as received. All of the solutions were prepared with ultrapure Milli-Q water (18.2 M Ω cm) from a Millipore Milli-Q system.

Preparation of AuNPs-tagged Anti PEAK1 Bioprobes

Bioconjugation of AuNPs to Anti PEAK1 was carried out through a simple physisorption method. Briefly, AuNPs-tagged Anti PEAK1 were synthesized by adding 10 μL of 20 μg/mL Anti PEAK1 solution in 0.01 M phosphate-buffered saline (PBS, pH 7.2) to 100 μL of 20 nm diameter AuNPs solution in PBS, followed by gentle mixing at 4 °C for 12 h. After mixing and centrifugation, the obtained AuNPs-tagged Anti PEAK1 was incubated with 0.5% bovine serum albumin (BSA) to block any possible remaining active sites to avoid any non-specific absorption. The prepared AuNPs-tagged Anti PEAK1 bioprobes were stored at 4 °C until use.

Data Analysis

Once an image of the paper-based detection zones was captured, average brightness of each detection zone was measured using the ImageJ software, distributed for free by NIH (<http://rsb.info.nih.gov/ij/download.html>). RGB images can be converted to the gray scale using the formula $\text{gray} = (\text{red} + \text{green} + \text{blue}) / 3$. The display range in ImageJ from minimum to maximum is scaled from 0 to 255 (8-bit). The brighter, the higher gray value is.

Figure S1.

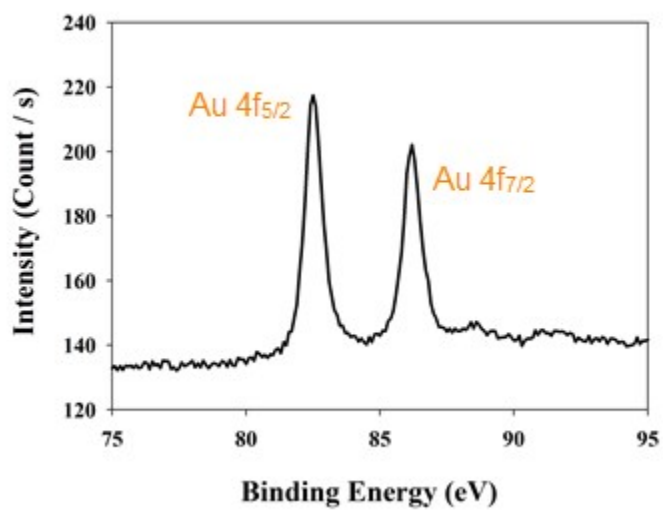


Figure S1. Deconvoluted Au 4f XPS spectra for the immunosensor.